Carbohydrate Polymers 178 (2017) 180–189

Contents lists available at ScienceDirect

Carbohydrate Polymers

journal homepage: www.elsevier.com/locate/carbpol

Molecular size is important for the safety and selective inhibition of intrinsic factor Xase for fucosylated chondroitin sulfate

Lufeng Yan[a], Junhui Li[a], Danli Wang[a], Tian Ding[a], Yaqin Hu[a], Xingqian Ye[a], Robert J. Linhardt[b], Shiguo Chen[a,*]

[a] Zhejiang University, College of Biosystems Engineering and Food Science, Zhejiang Key Laboratory for Agro-Food Processing, Fuli Institute of Food Science, Zhejiang R & D Center for Food Technology and Equipment, Hangzhou 310058, China

[b] Center for Biotechnology & Interdisciplinary Studies and Department of Chemistry & Chemical Biology, Rensselaer Polytechnic Institute, Biotechnology Center 4005, Troy, NY 12180, United States

ARTICLE INFO

Keywords:
Fucosylated chondroitin sulfate
N-deacetylation–deaminative cleavage
Anticoagulant activity
Intrinsic tenase complex inhibitor
Safe fragments

ABSTRACT

Fucosylated chondroitin sulfate from sea cucumber *Isostichopus badionotus* (FCS-*Ib*) showed potent anticoagulant activities without selectivity. The present study focused on developing safe FCS-*Ib* oligomers showing selective inhibition of intrinsic factor Xase (anti-FXase) prepared through partial *N*-deacetylation–deaminative cleavage. The *N*-deacetylation degree was regulated by reaction time, controlling the resulting oligomer distribution. Structure analysis confirmed the selectivity of degradation, and 12 high purity fractions with trisaccharide-repeating units were separated. *In vitro* anticoagulant assays indicated a decrease in molecular weight (*M*w) dramatically reduced activated partial thromboplastin time (APTT), thrombin time (TT), AT-dependent anti-FIIa and anti-FXa activities, while the oligomers retained potent anti-FXase activity until they fell below 3 kDa. Meanwhile, human FXII activation and platelet aggregation were markedly reduced with decreasing *M*w and were moderate when under 12.0 kDa. Thus, fragments of 3–12.0 kDa should be safe and effective as selective inhibitors of intrinsic tenase complex for application as clinical anticoagulants.

1. Introduction

Thrombotic disease has been the leading cause of death throughout the world (Mackman, 2008). Unfractionated heparin (UFH) and low molecular weight heparins (LMWHs) have been long-term and widespread use as anticoagulants. However, there can be serious bleeding risk in therapy using UFH and LMWHs due to the non-selectivity of their anticoagulant activity (Wu et al., 2015; Zhao et al., 2015). Fucosylated chondroitin sulfate (FCS) from sea cucumber has potent anticoagulant and antithrombotic activities essentially driven by serine protease inhibitor (serpin)-dependent and independent mechanisms (Glauser, Pereira, Monteiro, & Mourao, 2008; Nagase et al., 1995; Nagase et al., 1997; Sheehan & Walke, 2006). However, native FCS also causes undesirable side effects such as factor XII (FXII) activation and platelet aggregation (Chen et al., 2013; Wu et al., 2015; Zhao et al., 2015).

Fortunately, depolymerization has been considered to be an effective method to reduce these adverse effects, while maintaining anticoagulant activity similar to UFH and LMWHs (Wu et al., 2015). It has been reported that nonasacchairde (with three trisaccharide-repeating units) is the minimum fragment of depolymerized FCS that retains potent selective inhibition of the intrinsic factor Xase (anti-FXase) while avoiding the adverse effects of native FCS (Zhao et al., 2015). However, there has been no systematic evaluation of the specific molecular weight (*M*w) range required for selective targeting at intrinsic tenase complex with no severe adverse effects. This calls for the preparation of high-purity fragments of FCS oligomers of different molecular sizes.

Since there are no polysaccharide degrading enzymes that can digest FCS directly (Mourao et al., 1996), techniques for *M*w reduction of FCS have mainly focused on its chemical or physical degradation. However, acid-catalyzed hydrolysis can easily cause desulfation and destroy sulfated fucose branches (Gao, Wu, Li, & Chen, 2014), which are key components of FCS required for its anticoagulant activity (Mourao et al., 1996). Free-radical depolymerization is non-selective and it is hard to obtain pure oligomers in the *M*w range required for selective targeting at intrinsic tenase complex without exhibiting severe adverse effects (Wu, Xua, Zhao, Kang, & Ding, 2010; Yang et al., 2015).

Deaminative cleavage is a useful chemical method for depolymerizing heparin and heparan sulfate exhibiting high selectivity, since nitrous acid only acts on amino groups within the polysaccharides chain

* Corresponding author at: College of Biosystems Engineering and Food Science, Zhejiang University, Yuhangtang Road 866#, Hangzhou 310058, China.
E-mail address: chenshiguo210@163.com (S. Chen).

http://dx.doi.org/10.1016/j.carbpol.2017.09.034
Received 27 July 2017; Received in revised form 8 September 2017; Accepted 10 September 2017
Available online 12 September 2017
0144-8617/

(Petitou, 2003). Thus, based on the fact that hexosamines in FCS are all *N*-acetylated, a combination of hydrazine hydrate (for *N*-deacetylation) and nitrous acid has successfully depolymerized FCS (Zhao et al., 2015, 2013). Meanwhile, the *M*w of resulting fragments can be calculated using the formula: *M*w = 1/DD × 907, where DD is the *N*-deacetylation degree, and 907 is the *M*w of every constitutional FCS unit (Zhao et al., 2013). However, the specific oligomer distribution of resulting fragments from different DD needs to be clearly clarified, since the oligomer distribution is extremely important for anticoagulant activities and side effects (Liu et al., 2016; Wu et al., 2015). The separation and purification of individual depolymerized fragments is required for carrying out a detailed structure–activity relationship study.

In previous studies, we isolated pure FCS-*Ib* with high anticoagulant activity (Chen et al., 2013, 2011). Here we obtain a series of pure fragments with different *M*w by *N*-deacetylation–deaminative cleavage to compare their activities in prolonging activated partial thromboplastin time (APTT), prolonging thrombin time (TT), AT-dependent anti-FIIa and anti-FXa, anti-FXase, FXII activation and platelet aggregation. The aim of this study is to clarify the *M*w range required for both selective inhibition of intrinsic tenase complex and safety for further applications in clinical anticoagulation.

2. Materials and methods

2.1. Materials

FCS-*Ib* was isolated and purified from the sea cucumber *Isostichopus badionotus*. Isolation and purification of this polysaccharide were performed as previously described (Li et al., 2016). Hydrazine hydrate (containing about 64 wt.% hydrazine in water) and hydrazine sulfate were obtained from Aladdin Reagent (Shanghai, China). Sodium nitrite and deuterium oxide (D_2O) were obtained from Sinopharm Chemical Reagent Co., Ltd. (Shanghai, China). Unfractionated heparin (UFH), monosaccharides standards and adenosine diphosphate (ADP) were obtained from Sigma (St. Louis, MO, USA). LMWH (Enoxaparin, 0.4 mL × 4000 AXaIU) was obtained from Sanofi-Aventis (France). Activated partial thromboplastin time (APTT) assay kits, thrombin time (TT) assay kits, calcium chloride solution (0.02 M) and standard human plasma were obtained from MDC Hemostasis, Germany. Bovine antithrombin (AT), bovine FXa, bovine thrombin (FIIa), chromogenic substrate S-2765 and S-2238 were obtained from Adhoc International Technologies Co., Ltd, (Beijing, China). Human coagulation FVIII was obtained from China Biologic Products, Inc. (Shandong, China). Chromogenic assay kit for measuring FVIII: C in concentrates and kallikrein chromogenic substrate CS-31(02) were obtained from Hyphen Biomed (France). All other chemicals and reagents were of analytical grade.

2.2. FCS-Ib N-deacetylation

FCS-*Ib* *N*-deacetylation was performed using Fukuda's method with some modification (Fukuda, Kondo, & Osawa, 1976). Briefly, dried FCS-*Ib* (100 mg) and 1.50 mL hydrazine hydrate containing 1% hydrazine sulfate were added in a reaction tube. The tube was sealed and incubated at 90 °C for 12 h on a magnetic stirrer at 250 rpm. After the reaction, the solution was added to ethanol (quadruple the solution volume). When several drops of saturated sodium chloride were added, a white precipitate was formed. The precipitate was collected by centrifugation and dissolved in distilled water. This precipitation and dissolution procedure was repeated 4-times to remove the hydrazine and hydrazine sulfate. The resulting solution was dialyzed against flowing tap water for 2 d and distilled water for 1 d with a 3500 Da molecular weight cut-off and subsequently lyophilized.

To analyze the reaction conditions on *N*-deacetylated products, a series of experiments were performed based on the above representative protocol with varied reaction parameters (time, temperature, material-liquid ratio (w/v) and catalyst), and each experiment was performed at least in duplicate. In the protocol, the *N*-deacetylation degree (DD) of sample was calculated using the area ratio of two methyl peaks that were approximate 1.3 and 2.0 ppm in the ^1H NMR spectrum, which were from the *N*-acetylgalactosamine (GalNAc) methyl group and from the sulfated fucose (Fuc) methyl group, respectively. The *N*-deacetylated FCS-*Ib* yield was calculated using the weights of *N*-deacetylated and intact FCS-*Ib* sample.

2.3. N-deacetylated FCS-Ib deaminative cleavage

The deaminative cleavage was designed according to Bienkowski's method with some modifications (Bienkowski & Conrad, 1985). The nitrous acid reagent was prepared by mixture of 0.5 M H_2SO_4 and 5.5 M $NaNO_2$ at volume ratio of 3:5. In brief, 1 mL ice-cold 20 mg/mL *N*-deacetylated FCS-*Ib* solution was added to 2 mL pre-cooling nitrous acid reagent in a reaction tube. The reaction was performed for 10 min in an ice bath, and the excess nitrous acid was neutralized by addition of 1.5 mL 0.5 M NaOH. Immediately, 150 µL 300 mg/mL $NaBH_4$ (dissolved in 0.05 M NaOH) was added and reduced at 50 °C for 2 h. Finally, the sample was dialyzed with a 500 Da molecular weight cut-off and lyophilized as described above.

2.4. Composition analysis and molecular weight measurement

Monosaccharide composition was determined by the 1-phenyl-3-methyl-5-pyrazolone derivatization followed by high performance liquid chromatography (PMP-HPLC) (Wu et al., 2013). Sulfate content was measured with a BaCl2-Gelatin method (Dodgson & Price, 1962). Molecular weight measurement was determined by high performance gel permeation chromatography (HPGPC). The native, *N*-deacetylated and deaminative cleavage samples were performed on a Waters Ultrahydrogel 250 column (3.9 × 300 mm) (Milford, MA, USA) eluted by 0.2 M NaCl aqueous solution at the flow rate 0.5 mL/min monitored with a refractive index detector. Glucan standards were used to determine the *M*w of the samples. The oligomer distribution of deaminative cleavage samples were analyzed using a Superdex Peptide 10/300 GL column (10 × 300 mm) eluted by 0.2 M NaCl at the flow rate 0.4 mL/min monitored with a refractive index detector. HILIC LC ESI-LTQ-Orbitrap-FTMS analysis of deaminative cleavage sample was account for precise *M*w of oligomers while referring to Li et al. (Li et al., 2014).

2.5. Purification oligomers of depolymerized FCS-Ib

The mixed fragments of depolymerized FCS-*Ib* (47.6% DD) were fractionated by gel filtration on a Superdex 30 prep grade column (2.6 × 120 cm) eluted with 0.3 M NH_4HCO_3 at a flow rate of 0.3 mL/min, and were collected in a tube every 6 min. Every tube of sample was analyzed using a Waters Ultrahydrogel 250 column (3.9 × 300 mm) or a Superdex Peptide 10/300 GL column (10 mm × 300 mm) and monitored with a refractive index detector, those showed almost single peak were collected for further testing.

2.6. NMR spectroscopy

For NMR spectroscopic analysis, samples (30 mg) were dissolved in 500 µL of D_2O (99.9%) and lyophilized three times to substitute the exchangeable protons, and then dissolved in 500 µL D_2O containing 0.1 µL acetone, and finally transferred to NMR microtubes. In addition, ^1H, ^{13}C, ^1H-^1H COSY and ^1H/^{13}C HSQC NMR experiments were performed on a Hudson-Bruker SB 600 MHz Spectrometer (Madison, WI, USA) at room temperature.

2.7. Anticoagulant activity measurement

The activated partial thromboplastin time (APTT) and thrombin

time (TT) assays were determined with a coagulometer (RAC-120, China) using APTT and TT reagents and standard human plasma as previously described (Gao et al., 2012). The results were expressed as international units/mg using a parallel standard curve based on the International Heparin Standard (212 IU/mg).

Anti-thrombin (anti-FIIa) and anti-factor Xa (anti-FXa) activities in the presence of antithrombin (AT), and inhibition of intrinsic factor Xase (factor IX-factor VIIIa complex) in the presence of samples were carried out in a 96-well micro-titerplate as described (Wu et al., 2015). The absorbance change rate was proportional to the FIIa and FXa activity remaining in the incubation mixtures. The experimental results were expressed as the percent of control (n = 3). EC_{50} values were obtained by fitting the data to a noncompetitive inhibition model for the samples according to Sheehan and Walke (Sheehan & Walke, 2006).

2.8. Activation of human factor XII and platelet aggregation assays

The activation of human factor XII (FXII) in the presence of samples was determined by a previously described method (Fonseca et al., 2010; Wu et al., 2015). Turbidimetric measurement of platelet aggregation with samples was performed in a Pulisheng Model LBY-NJ4 Aggregometer (Pulisheng Corporation, Beijing, China), according to Born's method (Born, 1962). Changes in optical density as a result of platelet aggregation were recorded, and max aggregations in the presence of samples were compared.

3. Results and discussion

3.1. FCS-Ib N-deacetylation

The effects of reaction time, temperature as well as the material-liquid ratio and catalyst were investigated to optimize the FCS-*Ib* *N*-deacetylatation conditions (Table 1). The results indicated the DD increased in direct proportion to reaction time. FCS-*Ib* with different DD could be obtained by controlling the reaction time. The reduction in the *M*w of *N*-deacetylated product and the yields and content of glucuronic acid (GlcA) are presented in Table 1. These changes were caused by the β-elimination cleavage of FCS-*Ib* under alkaline condition, since the β-eliminative cleavage in heparan sulfate polymer chain using 70% hydrazine in water has been reported (Guo & Conrad, 1989). An increase of the polydispersity was also observed, which was also caused by the β-elimination cleavage.

Catalyst and high bath temperature were also necessary for accelerating the *N*-deacetylation of FCS-*Ib*. The results indicated that by adding hydrazine sulfate the *N*- deacetylation rate could be accelerated with a slight decrease in *M*w, compared to the same reaction in the absence of catalyst. Hydrazine sulfate is a commonly used catalyst in glycoprotein and glycosaminoglycan hydrazinolysis (Fukuda et al., 1976), provided protons to accelerate the *N*-deacetylation rate and avoided incomplete β-elimination. Increased reaction temperature resulted in increased DD, and ≥ 90 °C was considered to be an effective *N*-deacetylation temperature. The material-liquid ratio (w/v) could also influence the *N*-deacetylation rate, but its effect was much more subtle as doubling the hydrazine (containing 1% hydrazine sulfate) only increased DD by 10%. Meanwhile, sulfate content of FCS-*Ib* kept stable during *N*-deacetylation (Table 1), and this was appropriate for preparation of oligomers with complete structure.

3.2. FCS-Ib deaminative cleavage

The *N*-deacylated FCS provides the sites for the attack by the nitrous acid. We tested the deaminative cleavage products of all deacetylated FCS-*Ib* prepared using different *N*-deacetylation conditions by HPGPC and PAGE (some are shown in Fig. 1). HPGPC and PAGE analyses (Fig. 1) combining with the HILIC LC ESI-LTQ-Orbitrap-FTMS analysis (Supplementary Fig. S1) of depolymerized FCS-*Ib* showed that deaminative cleavage of FCS-*Ib* produced a series of fragments with trisaccharides-repeating units. All of these results were consistent with previous reports about basic structure of FCS, which had chondroitin sulfate-type backbone with large numbers of sulfated fucose side chains (Myron, Siddiquee, & Al Azad, 2014).

HPGPC profile analysis was performed to investigate the relationship between *N*-deacetylation conditions and the *M*w with oligomer distribution of depolymerized products (Table 2). The results revealed that the *M*w decreases along with the increasing deacetylation degree, as determined by reaction time. Meanwhile, *N*-deacetylation time determined the proportion of oligomers having different percentages of trisaccharide-repeating units. Insufficient *N*-deacetylation time resulted in dominant macromolecular products (> 18 mer) with wide oligomer distribution, while excessive *N*-deacetylation time resulted in smaller degradation products (< 9 mer). PAGE anylsis of depolymerized products using different *N*-deacetylation times are presented in Fig. 1C, and reflect the oligomer distributions intuitively. Similarly, the presence of catalyst and a high reaction temperature (> 90 °C) were necessary for appropriate DD, which resulted in smaller molecular size and narrower distribution of the degradation products. The material-liquid ratio (w/

Table 1
Effects of different *N*-deacetylation conditions on physicochemical properties of products.

N-Deacetylation conditions[a]		DD (%)	Mw (kDa)	Polydispersity (*M*w/*M*n)	Yields (%)	Molar ratio[b]			
						GalNAc	GlcA	Fuc	Sulfate
Intact		0	98.3	1.16	100	1	1.43	1.28	4.24
Reaction time (h)	6	33.2	70.9	1.35	91.7	1	1.33	1.27	4.18
	12	47.6	47	1.84	84.1	1	0.91	1.38	4.15
	18	55	31.2	1.82	80.8	1	0.87	1.36	3.98
	24	67.4	20.7	1.76	76.8	1	0.81	1.31	3.87
	30	75.7	15.8	1.5	68.1	1	0.76	1.41	4.12
	36	80.9	11.8	1.41	64.7	1	0.75	1.51	4.07
Material-liquid ratio (w/v) and catalyst	1:15 without catalyst	40.1	20.6	1.69	76.8	1	0.82	1.34	3.82
	1:10 with 1% catalyst	45.1	46.8	1.89	80.6	1	1.23	1.33	3.92
	1:15 with 1% catalyst	47.6	47	1.84	84.1	1	0.91	1.38	4.15
	1:20 with 1% catalyst	50.8	41.6	1.89	82.3	1	0.92	1.4	4.02
Reaction temperature (°C)	60	21.4	94.2	1.18	97.6	1	1.38	1.29	4.26
	75	32.7	88.4	1.27	92.8	1	1.35	1.28	4.18
	90	47.6	47.0	1.84	84.1	1	0.91	1.38	4.15

[a] The 100 mg dried FCS samples were hydrazinolyzed by 1.50 mL of hydrazine hydrate (indicated as 1:15 material-liquid ratio (w/v)) containing 1% (15 mg) hydrazine sulfate at 90 °C for 12 h, precipitated, dialyzed, lyophilized and determined by HPGPC and NMR. The conditions for hydrazinolysis were investigated as reaction time, material-liquid ratio, catalyst, and reaction temperature while varying levels of the variables in this table.

[b] The molar ratio of sugars and sulfate were compared by defining the GalNAc content as 1 molar.

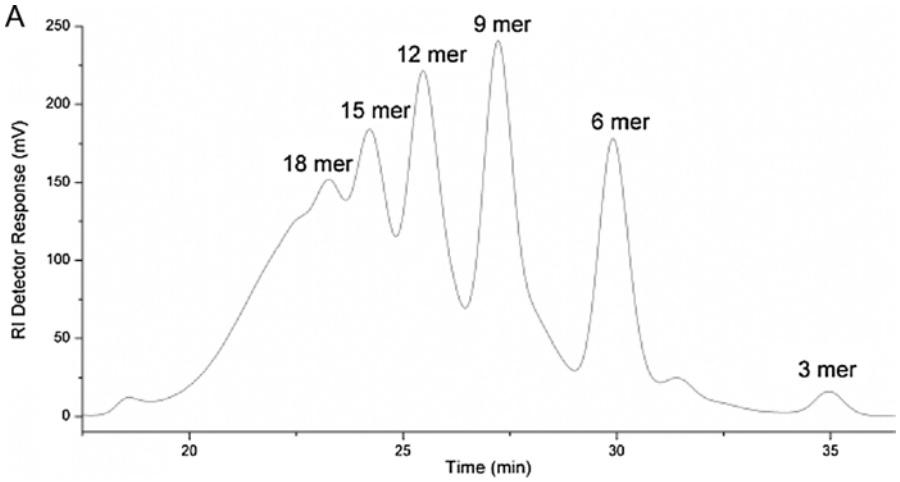

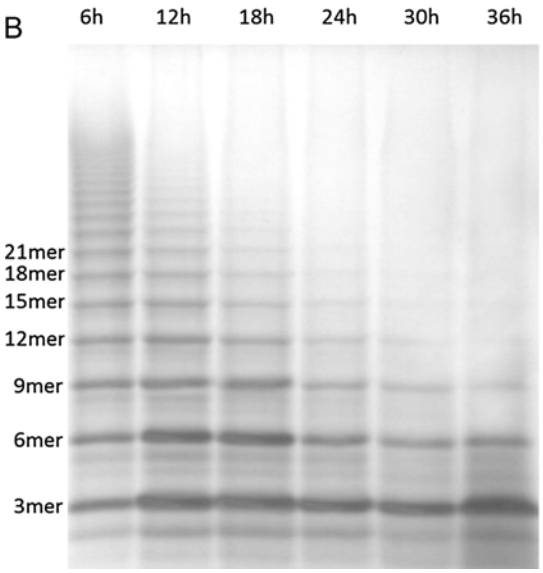

Fig. 1. (A) HPGPC profiles of depolymerized FCS-*Ib* (47.6% DD) by using a Superdex Peptide 10/300 GL column; (B) Polyacrylamide gel electrophoretograms (PAGE) of the depolymerized FCS-*Ib* from different *N*-deacetylation times, analyzed with a 22% gel (one trisaccharide unit = 3 mer).

Table 2
The *M*w and oligomer distribution of the depolymerized FCS-*Ib* by deaminative cleavage of different *N*-deacetylation conditions.

N-Deacetylation conditions		Mw (kDa)	Polydispersity (*M*w/*M*n)	Oligomer distribution[a]						
				3 mer	6 mer	9 mer	12 mer	15 mer	18 mer	> 18 mer
Reaction time (h)	6	10.6	1.33	0.93%	6.97%	10.93%	11.43%	13.47%	12.69%	43.57%
	12	7.36	1.19	1.30%	16.49%	21.46%	19.65%	15.53%	9.37%	16.20%
	18	5.44	1.22	3.14%	24.28%	26.42%	19.79%	10.67%	7.21%	8.48%
	24	5.15	1.19	3.95%	31.01%	29.72%	18.10%	7.92%	4.29%	5.00%
	30	4.45	1.18	16.80%	42.13%	24.77%	11.02%	3.97%	1.06%	0.26%
	36	4.42	1.17	10.27%	48.36%	26.93%	8.94%	2.83%	1.05%	1.63%
Material-liquid ratio (w/v) and catalyst	1:15 without catalyst	10.6	1.31	1.39%	8.86%	12.94%	12.85%	16.04%	12.85%	35.06%
	1:10 with 1% catalyst	8.43	1.22	1.46%	12.64%	17.33%	16.66%	14.28%	12.89%	24.75%
	1:15 with 1% catalyst	7.36	1.19	1.30%	16.49%	21.46%	19.65%	15.53%	9.37%	16.20%
	1:20 with 1% catalyst	6.9	1.28	2.73%	19.86%	23.31%	19.67%	13.43%	8.05%	12.96%
Reaction temperature (°C)	60	41.5	1.76	0.54%	1.73%	1.62%	1.62%	2.00%	2.91%	89.58%
	75	20.1	1.54	0.97%	4.24%	5.02%	6.38%	7.31%	7.84%	68.24%
	90	7.36	1.19	1.30%	16.49%	21.46%	19.65%	15.53%	9.37%	16.20%

[a] The oligomer distribution was determined by calculating the area ratio of fractionated peak on HPGPC profiles by using a Superdex Peptide 10/300 GL column.

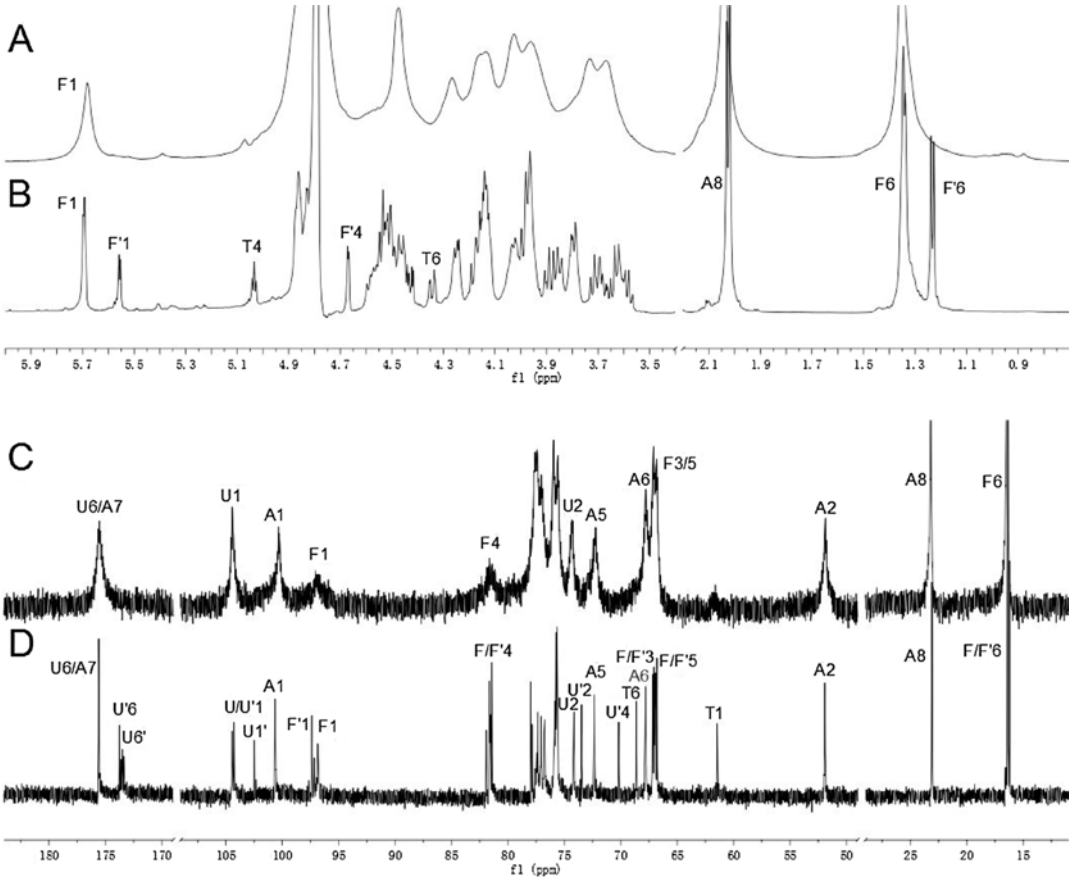

Fig. 2. Structural analysis of native and depolymerized FCS-*Ib* (47.6% DD): ^{1}H (A) and ^{13}C (C) NMR spectra of native FCS-*Ib*; ^{1}H (B), ^{13}C (D), ^{1}H-^{1}H COSY (E) and $^{1}H/^{13}C$ HSQC (F) NMR spectra of depolymerized FCS-*Ib* (47.6% DD). Labels U, F and A represent GlcA, Fuc and GalNAc residues, in the middle of the chains, respectively. Labels U' and F' represent GlcA and Fuc residues at new terminus of the chains, respectively, and label T represents an anTal-ol residue at the new reducing end.

v) had only moderate effect on *N*-deacetylation, as a result, it only had a small impact on the deaminative cleavage products. Thus, it is important to control the *N*-deacetylation time to prepare FCS oligomers of target molecular size having good anticoagulant activity and negligible side effects.

3.3. Structural analysis of native, N-deacetylated and depolymerized FCS-Ib

The *N*-deacetylated products (Supplementary Fig. S2) as well as the depolymerized fragments prepared by 47.6% DD with a narrow oligomer distribution were analyzed by NMR to investigate the mechanism of the degradation as well as the structure changes of the deaminative cleavage products (Fig. 2). The signals at 5.6–5.8 ppm, 1.9–2.1 ppm and 1.2–1.4 ppm in the ^{1}H NMR of the native FCS-*Ib* and *N*-deacetylated products (Supplementary Fig. S2) could be easily assigned to the H-1of 2,4-*O*-disulfated Fuc (Fuc2,4S), the methyl (CH_3) protons of GalNAc and Fuc. The signals of H-1 and H-6 for Fuc were partly shifted because of *N*-deacetylation. The new signal at 3.2–3.3 ppm was from H-2 of newly formed GalN by *N*-deacetylation of GalNAc. Meanwhile, the signal for the $-COCH_3$ group of GalNAc was reduced during *N*-deacetylation. Thus, degree of *N*-deacetylation could be reflected by comparing the signals for the $-COCH_3$ group of GalNAc and the CH_3 group of Fuc. Other signals had no obvious changes in chemical shits, suggesting that except *N*-deacetylation, the hydrazinolysis process had little impact on the structure of FCS-*Ib*, which was consistent with literature reports (Zhao et al., 2013).

Depolymerized FCS-*Ib* (47.6% DD) was also similar to the native FCS-*Ib* on structure by comparing their ^{1}H and ^{13}C NMR spectra (Fig. 2A–D). H-1 signal at approximate 5.70 ppm, and corresponding C-1 signal at approximate 96.5 ppm for Fuc2,4S, showed stable sulfated Fuc branches during *N*-deacetylation and deaminative cleavage. However, there were some obvious changes that could be observed after depolymerization. In the 1D spectrum, anTal-ol residue was found at the new reducing end by H-4 and H-6 signals at approximate 5.04 ppm and 4.36 ppm respectively, and C-1 signal at approximate 61.4 ppm, which was consistent with the literature. (Lauder, Huckerby, Nieduszynski, & Sadler, 2011; Tommeraas, Varum, Christensen, & Smidsrod, 2001; Zhao et al., 2015). The content of GlcA and Fuc residues at the terminus of the depolymerized chain increased through degradation. Thus, some of the GlcA and Fuc protons' signals were shifted. For example, new signals appeared around 5.56 ppm and 1.24 ppm, which could be assigned to H-1 and H-6 of Fuc2,4S residues at the terminus of the depolymerized chain. Correspondingly, in the ^{13}C NMR spectra, new signals appearing at around 97.3 ppm and 16.2 ppm could be assigned to C-1 and C-6 of these Fuc2,4S residues, respectively.

Since the signals of depolymerized FCS-*Ib* significantly overlapped in the 1D NMR spectra, the detailed signal assignment required 2D NMR, including correlation spectroscopy (COSY) (Fig. 2E) and heteronuclear single quantum coherence (HSQC) (Fig. 2F). Combining the results of 1D and 2D NMR spectra, some new signals could be assigned to new terminus of the depolymerized FCS-*Ib* as shown in Fig. 2. For the new terminal Fuc2,4S residues, the H-4 (4.68 ppm) and H-5 (4.53 ppm) were shifted more than H-2 (4.44 ppm) and H-3 (4.12 ppm) when compared to the middle Fuc2,4S residues, since the breakage of

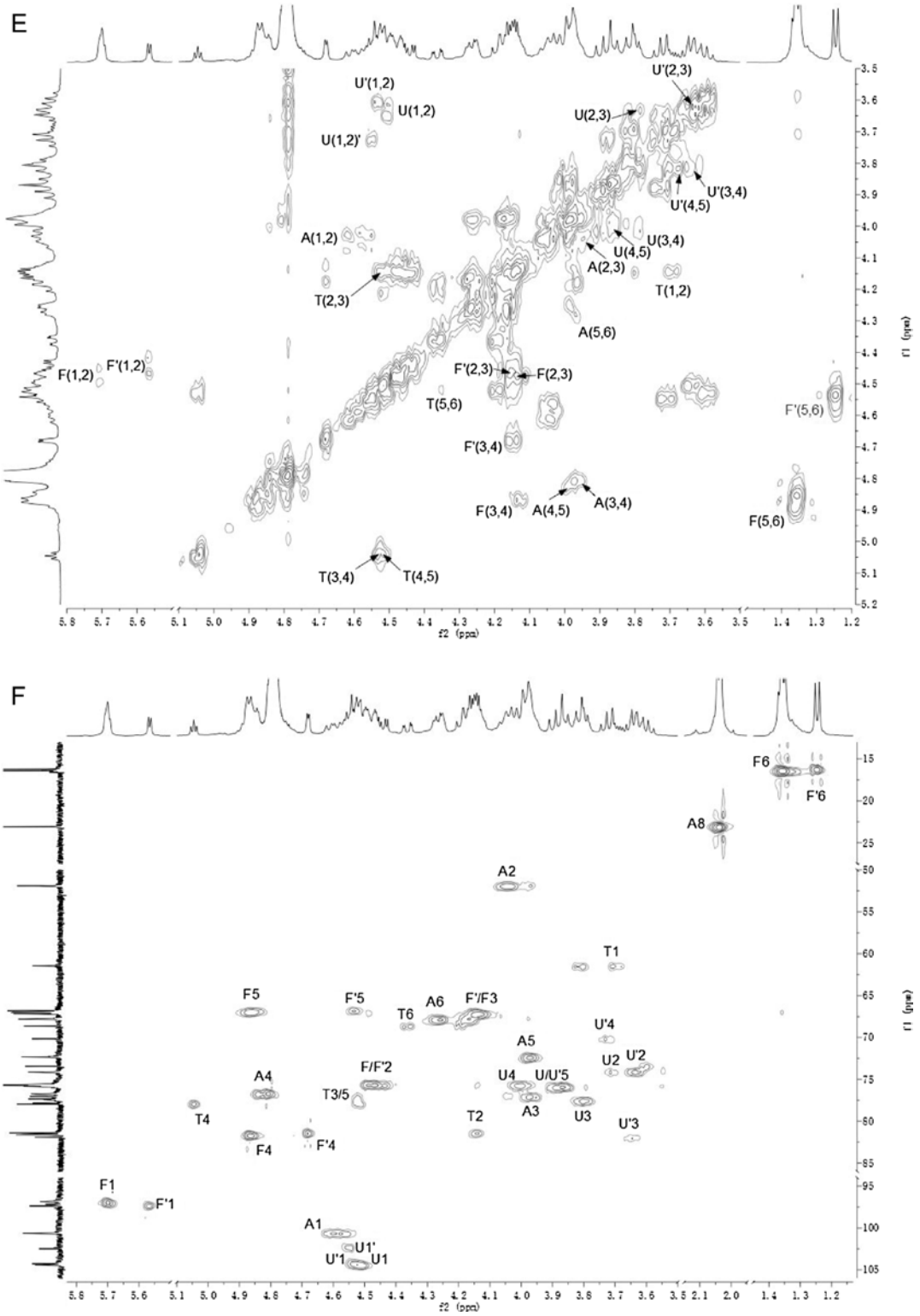

Fig. 2. (*continued*)

glycosidic linkage between GalNAc and GlcA had a greater effect on the chemical environments of H-4 and H-5. Similarly, for the new terminal GlcA residue, H-3 (3.65 ppm), H-4 (3.73 ppm) and C-3 (82.0 pm), C-4 (70.1 ppm) showed a greater shift than other protons and carbons because of the breakage of glycosidic linkage on C-4. In addition, H-1 (4.55 ppm) and C-1 (102.3 ppm) of middle GlcA residue were obviously shifted from other middle GlcA residue for linking to the new anTal-ol residue. There were obvious shifts in the signals for GalNAc, because

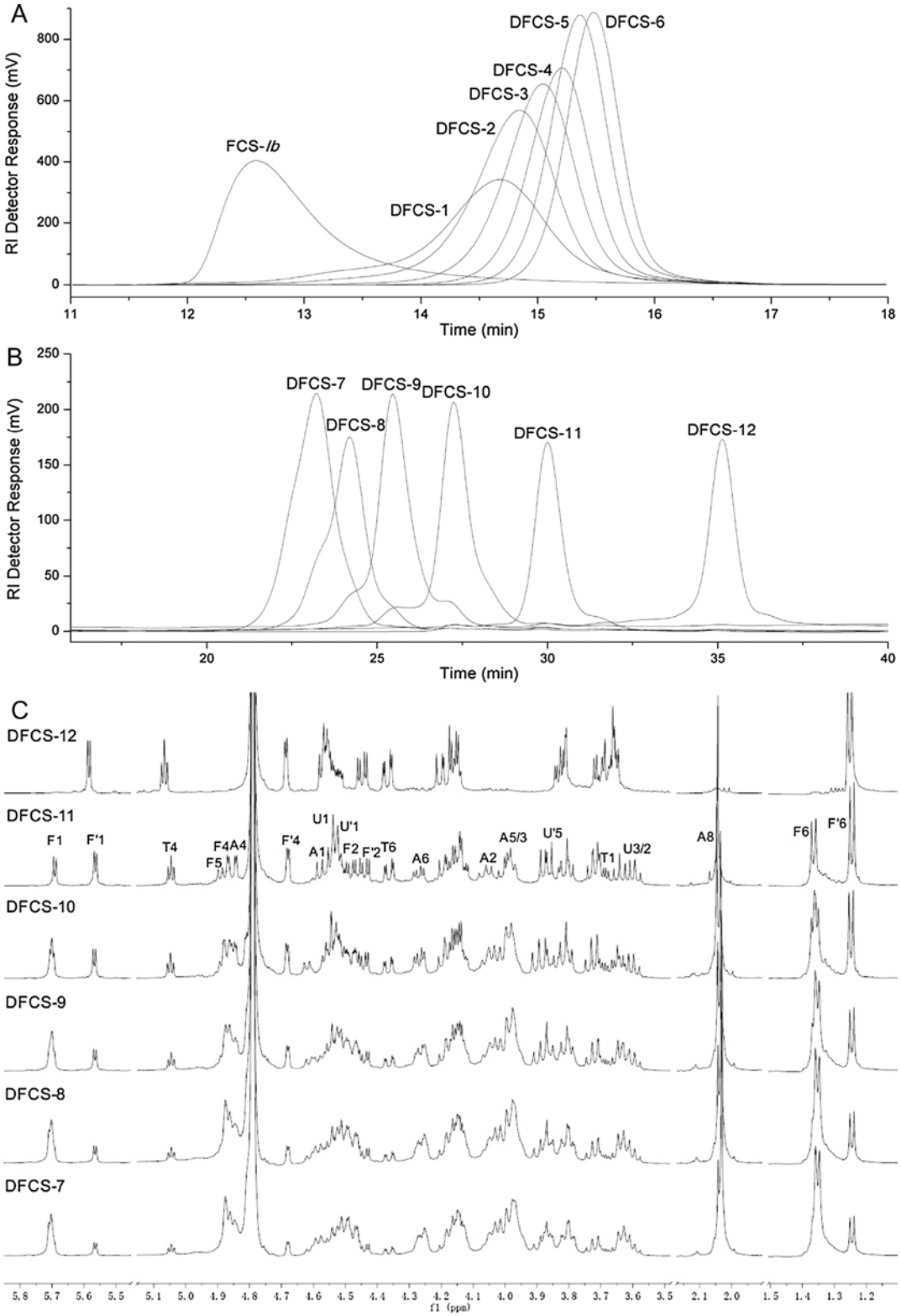

Fig. 3. (A) HPGPC profiles of native FCS-*Ib* and DFCS-1 to 6 by using a Waters Ultrahydrogel 250 column; (B) HPGPC profiles of DFCS-7 to 12 by using a Superdex Peptide 10/300 GL column; (C) ^{1}H NMR spectra of DFCS-12 to 7.

the terminal GalNAc had changed into anTal-ol residue and all GalNAc remained in middle of the chain. All the signals for the anTal-ol residue could be found in 2D NMR spectra. For example, the signals at 3.70, 4.14 ppm in ^{1}H and 61.4, 81.4 ppm in ^{13}C were assigned to the H-1, H-2 and C-1, C-2 of anTal-ol, respectively. Based on these analyses, ^{1}H and ^{13}C NMR signals of depolymerized FCS-*Ib* with native FCS-*Ib* (cited from reference (Chen et al., 2013; Li et al., 2017)) were assigned as demonstrated in Supplementary Table S1. In general, the depolymerization of FCS-*Ib* by deaminative cleavage had little effect on *O*-sulfo group substituents and the sulfated fucose branches as demonstrated by comparing the 1D and 2D NMR spectra of native and depolymerized FCS-*Ib*.

3.4. Structure analysis of purified FCS oligomers

To investigate the detailed structure changes of the FCS-*Ib* during depolymerization as well as the anticoagulant mechanism of the FCS-*Ib* oligomers, the mixed fragments of depolymerized FCS-*Ib* (47.6% DD) were further purified on a superdex 30 column (2.6 cm × 100 cm) and 12 fractions were obtained and named as DFCS-1 to 12 according their diminishing *M*w (Fig. 3A,B).

^{1}H NMR was used to investigate the detailed structure of pure FCS-*Ib* oligomers. ^{1}H NMR spectra of DFCS-7 to 12 were shown in Fig. 3C. DFCS-12, as a trisaccharide unit of L-Fuc2,4*S*-α1,3-D-GlcA-β1,3-D-anTal-ol, had on signals of GlcA, Fuc2,4S and GalNAc residues in the middle of the chains, while having intense signals of GlcA, Fuc2,4S and anTal-ol residues at terminus of the chains, compared with DFCS-11 to 7. As the chain grows, the proportion of GlcA, Fuc2,4S and anTal-ol at terminus of the chains are reduced. Thus, from DFCS-12 (3 mer) to DFCS-7 (18 mer), the signals of H-1 (5.55-5.58 ppm), H-4 (4.67-4.69 ppm) and H-6 (1.22-1.26 ppm) of terminal Fuc2,4S residues and the signals of H-4 (5.03-5.06 ppm) and H-6 (4.34-4.39 ppm) of anTal-ol were dramatically reduced. In addition, the area ratio of methyl peaks of Fuc2,4S residues in the middle (2.00-2.06 ppm) and at the terminus (1.22-1.26 ppm) of the chains accurately matched the trisaccharide-repeating units of DFCS-7 to 12. For example, DFCS-7, as a fragment of six trisaccharide-repeating units, its ratio value was 5.00, which was in accord with the structure of five middle Fuc2,4S residues and one terminal Fuc2,4S residue in a chain. Thus, this represented an accurate method for authenticating the degree of polymerization or precise *M*w of FCS fragments prepared by partial deacetylation–deaminative cleavage.

3.5. Anticoagulant properties of depolymerized fragments DFCS 1-12

To investigate the effect of the molecular size on the selective targeting intrinsic tenase complex of the FCS-*Ib* oligomers, the high purity oligomers named as DFCS-1 to 12 were obtained to compare their anticoagulant properties with native FCS-*Ib*, UFH and LMWH (enoxaparin), including APTT, TT, anti-FIIa/AT, anti-FXa/AT and anti-FXase. The results indicated the *M*w of depolymerized fragments were important to anticoagulant activity of FCS-*Ib* (Table 3 & Supplementary Fig. S3 & S4). The concentrations required for doubling APTT and TT increased obviously with decrease of *M*w, which accorded with the consequence of depolymerized FCS from sea cucumber *Thelenota ananas* and sea cucumber *Apostichopus japonicas* by free radical depolymerized methods in the literature (Wu et al., 2015; Yang et al., 2015). The TT prolongation almost disappeared after the size of the oligomers reducing to 12.0 kDa. Comparing to APTT, TT was more affected by a decrease in *M*w. The APTT assay determines interference with the intrinsic coagulation cascade and the TT assay examined the last step of the coagulation cascade, thrombin-mediated fibrin formation (Lin et al., 2007). This suggests that a decrease in the molecular size of fragments can result a selective targeting of intrinsic pathway for anticoagulant properties, although the detail mechanism still needs to be determined by other methods.

The inhibition of FIIa and FXa by AT and FXase were investigated and compared with native FCS-*Ib*, UFH and LMWH (Supplementary Fig. S4) to clarify the further anticoagulant properties and mechanism of different *M*w depolymerized FCS-*Ib* fragments. The results indicated that all the activities of these samples were concentration-dependent and their intensity decreased with decreasing *M*w. However, for AT-dependent anti-FIIa and anti-FXa activities, the latter decreased less with decreasing *M*w. For instance, AT-dependent anti-FXa activity of DFCS-6 (9.52 IU/mg) was about 8-times the AT-dependent anti-FIIa activity of DFCS-6 (1.23 IU/mg) although the native FCS-*Ib* had weaker intensity in AT-dependent anti-FXa than anti-FIIa activities. The obviously reducing ability of low *M*w FCS-*Ib* fragments to inactivate FIIa by AT was likely due to their monophasic-binding affinity to AT and might not have an allosteric activation effect on AT binding to FIIa (Xiao et al., 2016). When *M*w decreased to lower than 12.0 kDa, the binding properties were very weak. In general, the intensity ratio of anti-FXa and anti-FIIa by AT increased along with decreasing *M*w for FCS-*Ib*, and this was distinctly important in reducing side effects such as bleeding (Kitazato, Kitazato, Sasaki, Minamiguchi, & Nagase, 2003).

Additionally, the native FCS-*Ib* (334 IU/mg) was much more effective in inhibition of intrinsic factor Xase (factor IX-factor VIIIa complex) than UFH (212 IU/mg) and LMWH (42.4 IU/mg), suggesting the potential specific targeting for intrinsic pathways. The anti-FXase activity decreased less with decreasing *M*w than any other anticoagulant properties (Table 3 & Supplementary Fig. S4). When *M*w decreased to less than 12.0 kDa, the fragments exhibited powerful anti-FXase activity with weak anti-FXa/AT activity and negligible anti-FIIa/AT activity. As the *M*w continued to decrease, anti-FXase activity remained much more stable than the anti-FXa/AT activity. Low *M*w FCS-*Ib* fragments were effective intrinsic tenase complex inhibitors until molecular size was reduced to 9 mer, after which they lost activity for the inhibition of FIIa and FXa by AT. These results were consistent with previous reports that 9 mer was the minimum effective oligomer for selective inhibition of the intrinsic coagulation pathway (Zhao et al., 2015), the final and rate-limiting enzyme complex without risk for causing serious bleeding. In conclusion, with the decrease of *M*w, depolymerized fragments reduced anticoagulant property; however, their anticoagulant mechanism became simplified at the same time. This showed that fragments of *M*w from 3 kDa (9 mer) to 12.0 kDa showed great selectivity in inhibiting generation of FXa.

3.6. Safety evaluation of depolymerized fragments DFCS-1 to 12

The most notable side effects for native FCS were platelet aggregation and FXII activation that could result in hypotension (Chen et al., 2013; Fonseca, Santos, & Mourao, 2009). Thus, FXII activation and platelet aggregation of DFCS 1-12 were evaluated to ensure the safe *M*w range for avoiding these side effects (Fig. 4), by comparing with native FCS-*Ib*, UFH and LMWH (enoxaparin). Notably, the native FCS-*Ib* greatly activated FXII, while UFH and LMWH showed only a moderate effect, and LMWH showed the lowest activation of FXII. Comparison among the activation of FXII by native FCS-*Ib* and depolymerized fragments suggested that the activation was reduced with decreasing *M*w, especially at concentrations < 16 μg/mL (Fig. 4A). When *M*w was reduced to below 12.0 kDa (DFCS-5 to 12), FXII activation was below or close to that of UFH, which was consistent with previous reports on depolymerized FCS by free radical degradation (Wu et al., 2015).

Similarly, a decrease in the *M*w of FCS-*Ib* fragments also reduced platelet aggregation, as investigated using a conventional turbidimetric assay. Aggregation was quantified and recorded by changes in optical density, and max aggregations in the presence of ADP and different samples were compared (Fig. 4B). Native FCS-*Ib* caused significant platelet aggregation in citrated human PRP (30 μg/mL), which was almost the same as ADP (10 μM). When *M*w was less than 12.0 kDa, samples (DFCS-5 to 12) did not induce significant platelet aggregation at a concentration of 30 μg/mL, which was close to or below the effect

Table 3
Anticoagulant properties of DFCS 1-12.

Compd.	Mw[a] (kDa)	APTT		TT		anti-FIIa/AT		anti-FXa/AT		anti-FXase	
		μg/mL[b]	IU/mg[c]	μg/mL[b]	IU/mg[c]	μg/mL[d]	IU/mg[c]	μg/mL[d]	IU/mg[c]	μg/mL[d]	IU/mg[c]
FCS-Ib	98.3	16.6	153	12.3	152	4.10	28.4	4.90	13.4	0.19	334
DFCS-1	23.6	29.1	87.4	21.5	86.7	5.00	23.3	5.00	13.1	0.20	318
DFCS-2	19.5	28.9	87.9	27.1	69	5.90	19.8	5.10	12.9	0.22	289
DFCS-3	15.7	36.3	70.0	45.6	41	7.00	16.7	5.90	11.1	0.25	254
DFCS-4	13.6	32.8	77.4	~128	~14.6	8.00	14.6	6.10	10.8	0.26	244
DFCS-5	12.0	38.6	65.8	> 128	< 14.6	14.0	8.33	6.80	9.66	0.27	236
DFCS-6	10.8	39.8	63.9	> 128	< 14.6	95.0	1.23	6.90	9.52	0.30	212
DFCS-7	18 mer	46.5	54.7	> 128	< 14.6	180	< 1.00	7.50	8.76	0.33	192
DFCS-8	15 mer	62.7	40.5	> 128	< 14.6	> 1000	< 1.00	15.0	4.38	0.51	124
DFCS-9	12 mer	97.7	26.0	> 256	< 7.30	> 1000	< 1.00	40.0	1.63	0.91	69.9
DFCS-10	9 mer	160	15.8	> 256	< 7.30	> 1000	< 1.00	300	< 1.00	1.40	45.4
DFCS-11	6 mer	> 256	~7.00	> 512	< 3.65	> 1000	< 1.00	> 1000	< 1.00	15.0	4.24
DFCS-12	3 mer	> 512	~1.00	> 512	< 3.65	> 1000	< 1.00	> 1000	< 1.00	> 1000	< 1.00
UFH	~18.0	12.0	212	8.81	212	0.55	212	0.31	212	0.30	212
LMWH	~4.50	36.5	69.6	33.1	56.4	1.80	64.8	0.60	110	1.30	48.9

[a] The *M*w of FCS-*Ib*, DFCS-1 to 6, UFH and LMWH were determined by HPGPC. The *M*w of DFCS-7 to 12 were expressed as different polymerized trisaccharide-repeating units according to Figs. 1 A & 3 B.
[b] The concentration required to double the APTT/TT of human plasma (APTT/TT doubling).
[c] The activity is expressed as international units/mg using a parallel standard curve based on the International Heparin Standard (212 IU/mg).
[d] IC_{50} value, the concentration required to inhibit 50% of protease activity.

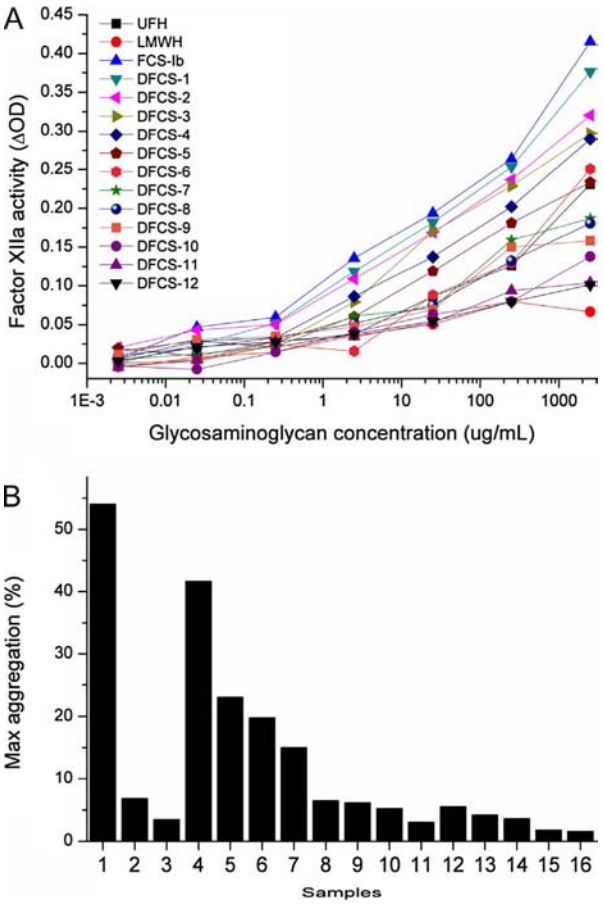

Fig. 4. Safety evaluation of the depolymerized fragments DFCS-1 to 12: (A) FXII activation in the presence of UFH, LMWH, FCS-*Ib* and DFCS-1 to 12; (B) Platelet aggregation induced by ADP, UFH, LMWH, FCS-*Ib* and DFCS-1 to 12. Labels 1, 2, 3, 4 and 5-16 represent ADP, UFH, LMWH, FCS-*Ib* and DFCS 1-12, respectively. The platelet aggregation was performed at 30 μg/mL of concentration of these samples in comparison to ADP (10 μM).

of UFH.

Together with results from anticoagulant assays, we can conclude that in a molecular size range between 3 kDa (9 mer) to 12.0 kDa, the FCS-*Ib* fragments can selectively target the intrinsic pathway, while only moderately activating FXII and platelet aggregation, which suggests their safe anticoagulant use in this *M*w range. Thus, the best extent of partial *N*-deacetylation–deaminative cleavage affording a DD around 47.6% to 55.0% would produce maximum amount of FCS-*Ib* fragments in the range recommended for the production of FCS-*Ib* fragments anticoagulants.

4. Conclusion

In the present study, we first investigated the effects of different deacetylation conditions on deacetylated products and deaminative cleavage products of fucosylated chondroitin sulfate from sea cucumber *Isostichopus badionotus*. The results showed that the fine structures of FCS-*Ib* oligomers were stable during these reactions and oligosaccharides with trisaccharide-repeating units were obtained. These *N*-deacetylation conditions for FCS-*Ib* produced a distribution of oligomer fragments, which were useful in producing oligomers with targeted *M*w. The anticoagulant activities and side effects of 12 highly purified FCS oligomers suggested a range of 3–12.0 kDa resulted in very intrinsic FXase inhibition with greatly reduced common side effects compared to UFH. Thus, a DD range from 47.6% to 55.0% is suggested for the production FCS-*Ib* oligomers having safe and selective targeting.

Acknowledgment

This work was supported by National Science Foundation of China (31301417) and by grants from the China Scholarship Council.

Appendix A. Supplementary data

Supplementary data associated with this article can be found, in the online version, at http://dx.doi.org/10.1016/j.carbpol.2017.09.034.

References

Bienkowski, M. J., & Conrad, H. E. (1985). Structural characterization of the oligosaccharides formed by depolymerization of heparin with nitrous-acid. *Journal of Biological Chemistry, 260*(1), 356–365.

Born, G. V. R. (1962). Aggregation of blood platelets by adenosine diphosphate and its reversal. *Nature, 194*(4832) [927- &].
Chen, S. G., Xue, C. H., Yin, L. A., Tang, Q. J., Yu, G. L., & Chai, W. G. (2011). Comparison of structures and anticoagulant activities of fucosylated chondroitin sulfates from different sea cucumbers. *Carbohydr Polym, 83*(2), 688–696.
Chen, S., Li, G., Wu, N., Guo, X., Liao, N., Ye, X., et al. (2013). Sulfation pattern of the fucose branch is important for the anticoagulant and antithrombotic activities of fucosylated chondroitin sulfates. *Biochimica et Biophysica Acta, 1830*(4), 3054–3066.
Dodgson, K. S., & Price, R. G. (1962). A note on the determination of the ester sulphate content of sulphated polysaccharides. *Biochemical Journal, 84*(1), 106–110.
Fonseca, R. J. C., Santos, G. R. C., & Mourao, P. A. S. (2009). Effects of polysaccharides enriched in 2, 4-disulfated fucose units on coagulation, thrombosis and bleeding Practical and conceptual implications. *Thrombosis and Haemostasis, 102*(5), 829–836.
Fonseca, R. J. C., Oliveira, S. N. M. C. G., Pomin, V. H., Mecawi, A. S., Araujo, I. G., & Mourao, P. A. S. (2010). Effects of oversulfated and fucosylated chondroitin sulfates on coagulation Challenges for the study of anticoagulant polysaccharides. *Thrombosis and Haemostasis, 103*(5), 994–1004.
Fukuda, M., Kondo, T., & Osawa, T. (1976). Studies on hydrazinolysis of glycoproteins – core structures of oligosaccharides obtained from porcine thyroglobulin and pineapple stem bromelain. *Journal of Biochemistry, 80*(6), 1223–1232.
Gao, N., Wu, M., Liu, S., Lian, W., Li, Z., & Zhao, J. (2012). Preparation and characterization of O-acylated fucosylated chondroitin sulfate from sea cucumber. *Marine Drugs, 10*(8), 1647–1661.
Gao, R. C., Wu, N., Li, Y., & Chen, S. G. (2014). Structures and anticoagulant activities of the partially mild acidic hydrolysis products of the fucosylated chondroitin sulfate from sea cucumber pearsonothuria graeffei. *Journal of Carbohydrate Chemistry, 33*(9), 471–488.
Glauser, B. F., Pereira, M. S., Monteiro, R. Q., & Mourao, P. A. S. (2008). Serpin-independent anticoagulant activity of a fucosylated chondroitin sulfate. *Thrombosis and Haemostasis, 100*(3), 420–428.
Guo, Y., & Conrad, H. E. (1989). The disaccharide composition of heparins and heparan sulfates. *Analytical Biochemistry, 176*(1), 96–104.
Kitazato, K., Kitazato, K. T., Sasaki, E., Minamiguchi, K., & Nagase, H. (2003). Prolonged bleeding time induced by anticoagulant glycosaminoglycans in dogs is associated with the inhibition of thrombin-induced platelet aggregation. *Thrombosis Research, 112*(1–2), 83–91.
Lauder, R. M., Huckerby, T. N., Nieduszynski, I. A., & Sadler, I. H. (2011). Characterisation of oligosaccharides from the chondroitin/dermatan sulphates: H-1 and C-13 NMR studies of oligosaccharides generated by nitrous acid depolymerisation. *Carbohydrate Research, 346*(14), 2222–2227.
Li, G. Y., Steppich, J., Wang, Z. Y., Sun, Y., Xue, C. H., Linhardt, R. J., et al. (2014). Bottom-up low molecular weight heparin analysis using liquid chromatography-Fourier transform mass spectrometry for extensive characterization. *Analytical Chemistry, 86*(13), 6626–6632.
Li, J. H., Li, S., Zhi, Z. J., Yan, L. F., Ye, X. Q., Ding, T., et al. (2016). Depolymerization of fucosylated chondroitin sulfate with a modified fenton-System and anticoagulant activity of the resulting fragments. *Marine Drugs, 14*(9).
Li, J., Li, S., Yan, L., Ding, T., Linhardt, R. J., Yu, Y., et al. (2017). Fucosylated chondroitin sulfate oligosaccharides exert anticoagulant activity by targeting at intrinsic tenase complex with low FXII activation: importance of sulfation pattern and molecular size. *European Journal of Medicinal Chemistry, 139*, 191–200.
Lin, C. Z., Guan, H. S., Li, H. H., Yu, G. L., Gu, C. X., & Li, G. Q. (2007). The influence of molecular mass of sulfated propylene glycol ester of low-molecular-weight alginate on anticoagulant activities. *European Polymer Journal, 43*(7), 3009–3015.
Liu, X., Hao, J., Shan, X., Zhang, X., Zhao, X., Li, Q., et al. (2016). Antithrombotic activities of fucosylated chondroitin sulfates and their depolymerized fragments from two sea cucumbers. *Carbohydrate Polymers, 152*, 343–350.
Mackman, N. (2008). Triggers, targets and treatments for thrombosis. *Nature, 451*(7181), 914–918.
Mourao, P. A. S., Pereira, M. S., Pavao, M. S. G., Mulloy, B., Tollefsen, D. M., Mowinckel, M. C., et al. (1996). Structure and anticoagulant activity of a fucosylated chondroitin sulfate from echinoderm – Sulfated fucose branches on the polysaccharide account for its high anticoagulant action. *Journal of Biological Chemistry, 271*(39), 23973–23984.
Myron, P., Siddiquee, S., & Al Azad, S. (2014). Fucosylated chondroitin sulfate diversity in sea cucumbers: a review. *Carbohydrate Polymers, 112*, 173–178.
Nagase, H., Enjyoji, K., Minamiguchi, K., Kitazato, K. T., Kitazato, K., Saito, H., et al. (1995). Depolymerized holothurian glycosaminoglycan with novel anticoagulant actions – Antithrombin-Iii-Independent and heparin-Cofactor-Ii-Independent inhibition of factor-X activation by factor-Ixa factor-Viiia complex and heparin-Cofactor-Ii-Dependent inhibition of thrombin. *Blood, 85*(6), 1527–1534.
Nagase, H., Kitazato, K. T., Sasaki, E., Hattori, M., Kitazato, K., & Saito, H. (1997). Antithrombin III-independent effect of depolymerized holothurian glycosaminoglycan (DHG) on acute thromboembolism in mice. *Thrombosis and Haemostasis, 77*(2), 399–402.
Petitou, M. (2003). 1976-1983, a critical period in the history of heparin: The discoveryof the antithrombin binding site. *Biochimie, 85*(1–2), 83–89.
Sheehan, J. P., & Walke, E. N. (2006). Depolymerized holothurian glycosaminoglycan and heparin inhibit the intrinsic tenase complex by a common antithrombin-independent mechanism. *Blood, 107*(10), 3876–3882.
Tommeraas, K., Varum, K. M., Christensen, B. E., & Smidsrod, O. (2001). Preparation and characterisation of oligosaccharides produced by nitrous acid depolymerisation of chitosans. *Carbohydrate Research, 333*(2), 137–144.
Wu, M. Y., Xua, S. M., Zhao, J. H., Kang, H., & Ding, H. (2010). Physicochemical characteristics and anticoagulant activities of low molecular weight fractions by free-radical depolymerization of a fucosylated chondroitin sulphate from sea cucumber Thelenata ananas. *Food Chemistry, 122*(3), 716–723.
Wu, N., Ye, X. Q., Guo, X., Liao, N. B., Yin, X. Z., Hu, Y. Q., et al. (2013). Depolymerization of fucosylated chondroitin sulfate from sea cucumber, Pearsonothuria graeffei, via Co-60 irradiation. *Carbohydrate Polymers, 93*(2), 604–614.
Wu, M., Wen, D., Gao, N., Xiao, C., Yang, L., Xu, L., et al. (2015). Anticoagulant and antithrombotic evaluation of native fucosylated chondroitin sulfates and their derivatives as selective inhibitors of intrinsic factor Xase. *European Journal of Medicinal Chemistry, 92*, 257–269.
Xiao, C., Lian, W., Zhou, L., Gao, N., Xu, L., Chen, J., et al. (2016). Interactions between depolymerized fucosylated glycosaminoglycan and coagulation proteases or inhibitors. *Thrombosis Research, 146*, 59–68.
Yang, J., Wang, Y., Jiang, T., Lv, L., Zhang, B., & Lv, Z. (2015). Depolymerized glycosaminoglycan and its anticoagulant activities from sea cucumber Apostichopus japonicus. *International Journal of Biological Macromolecules, 72*, 699–705.
Zhao, L., Wu, M., Xiao, C., Yang, L., Zhou, L., Gao, N., et al. (2015). Discovery of an intrinsic tenase complex inhibitor: Pure nonasaccharide from fucosylated glycosaminoglycan. *Proceedings of the National Academy of Sciences of the United States of America, 112*(27), 8284–8289.
Zhao, L. Y., Lai, S. S., Huang, R., Wu, M. Y., Gao, N., Xu, L., et al. (2013). Structure and anticoagulant activity of fucosylated glycosaminoglycan degraded by deaminative cleavage. *Carbohydrate Polymers, 98*(2), 1514–1523.